ISBN: 978-3-95450-261-5 ISSN: 2673-7000 doi: 10.18429/JACoW-NAPAC2025-THP062

PHYSICS MODEL TO STUDY RESONANT COMPTON SCATTERING*

W. Delooze†, Y. K. Wu
FEL Laboratory, TUNL, and Department of Physics, Duke University, Durham, NC, USA

Abstract

Over the past several decades, the elastic interaction between photons and electrons known as Compton scattering, has been the foundational mechanism for generating high-energy photon beams, particularly in the gamma-ray regime. Resonant interactions between photons and atomic systems offer significantly enhanced resonant cross-sections, often several orders of magnitude greater than what is achievable through conventional Compton scattering of electron and photon beams. The Gamma Factory initiative at CERN aims to exploit this enhancement by employing ultra-relativistic, partially stripped ion beams to generate high-intensity gamma-ray beams. In this work, we first examine the energy-matching requirements for resonance. We then present a semi-classical model based on a damped-driven oscillator to describe resonant Compton scattering. This model provides physical insight into the resonant cross-section and the limitations imposed by beam-beam interactions. We also propose a framework for simulating the scattering process.

INTRODUCTION

In 1923, Arthur Compton discovered the elastic scattering of photons by electrons, now known as Compton scattering. In this experiment, energy and momentum were transferred from the photon to the electron, resulting in an increase of x-ray wavelength after scattering from graphite [1]. Following the emergence of charged particle accelerators in the 1960s, interest grew in using relativistic electrons to reverse the direction of the energy exchange, producing a high-energy photon beam. Today, high-intensity light source facilities worldwide utilize Compton scattering to generate real x-ray and gamma-ray beams employed in various fields. For example, the nearly monochromatic and highly polarized gamma beam at the High Intensity Gamma-ray Source (HIGS) facility supports research in particle physics, nuclear physics, and astrophysics [2].

While these machines are capable of producing intense and energetic gamma-ray beams, they remain limited by the very small Thomson cross-section, $\sigma_T \approx 6.65 \times 10^{-29}$ m^2. This limitation can be overcome by using resonant Compton scattering, where photons interact with electrons bound by relativistic atomic systems in which resonance arises from internal transitions. The Gamma Factory (GF) [3, 4] is a proposed future Compton gamma source (CGS) at CERN that aims to exploit this resonant process. The primary goal of the GF is to generate intense, polarized gamma-ray beams with energies ranging from 1–400 MeV and a total flux that is several orders of magnitude greater than what is achievable with conventional CGSs. The GF has the potential to make a significant contribution to many different sub-fields of physics [3, 4].

KINEMATICS OF SCATTERING

We start with the conventional Compton scattering of a photon and an electron, as shown in Fig. 1, [5]. The 4-momentum conservation yields the scattered photon energy:

$$E_\gamma = \frac{\hbar\omega(1 - \beta\cos\theta_i)}{1 - \beta\cos\theta_f + \frac{\hbar\omega}{\gamma mc^2}(1 - \cos\theta_{\rm ph})}, \quad (1)$$

where θ_i is the angle between the incident photon and incident electron, θ_f is the angle between the scattered photon and the incident electron, and $\theta_{\rm ph} = \theta_i - \theta_f$ is the angle between the incident and scattered photons. The scattered photon energy is maximized for the head-on backscattering case:

$$E_\gamma = \gamma^2(1 + \beta)^2\hbar\omega, \quad (2)$$

where $\theta_i = \pi$ and $\theta_f = 0$.

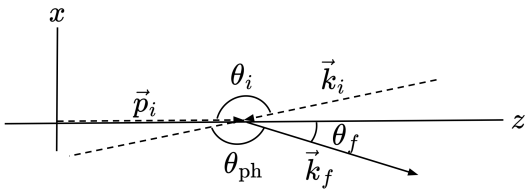

Figure 1: The collision scheme for Compton scattering.

In contrast, resonant Compton scattering differs in a few important ways. For a simple two-state system with a ground state and an excited state, the condition for resonant scattering requires that the energy of the photon in the ion rest frame matches the energy level difference (ΔE) between the two states:

$$\hbar\omega' = \Delta E = E_{\rm excited} - E_{\rm ground}. \quad (3)$$

For head-on collisions, this constrains the laser wavelength:

$$\lambda = 2\pi\gamma(1 + \beta)\frac{\hbar c}{\Delta E}, \quad (4)$$

where λ is the wavelength of the laser in the laboratory frame.

Figure 2 shows the required relationship between λ and γ for resonant scattering over a range of maximum scattered gamma-ray energies. A wide range of gamma-ray energies is accessible by selecting different ion species while tuning the

* This research is supported in part by the U.S. Department of Energy under Grant No. DE-FG02-97ER41033.
† william.delooze@duke.edu

ISBN: 978-3-95450-261-5 ISSN: 2673-7000 doi: 10.18429/JACoW-NAPAC2025-THP062

laser wavelength and/or ion energy. The background shading indicates the feasibility of achieving high laser power in each wavelength region. For instance, wavelengths below 200 nm are shaded in red to reflect the increased difficulty of generating a high-power laser beam in the deep UV, compared to the visible and IR.

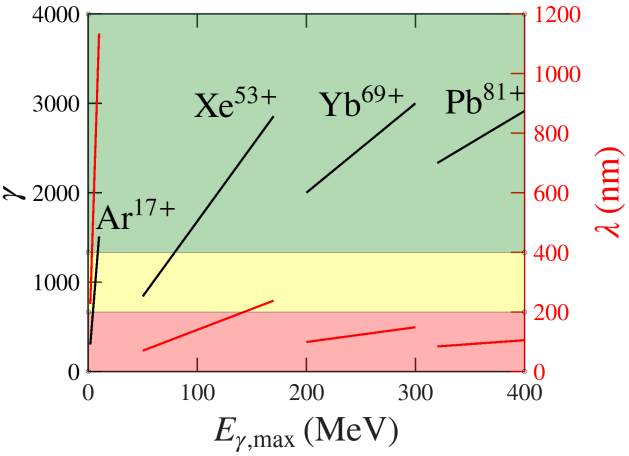

Figure 2: Coverage of maximum gamma-ray energies as a function of γ (black) and λ (red). Plotted lines correspond to the 2P→1S transition energy of different hydrogen-like ions. The background color indicates the relative difficulty of generating high-power laser light at each wavelength.

In the high gamma-ray energy region, around 320–400 MeV, Pb^{81+} can be used with γ ranging from 2300–2900, approaching the energy limits of the LHC [6,7]. The required laser wavelength is between 83–105 nm. While the laser need not be widely tuneable in this range, achieving a high laser power below 100 nm remains challenging.

In the low gamma-ray energy region, around 2–10 MeV, Ar^{17+} can be used with γ ranging from 300–1500, achievable by varying the accelerator energy. This requires a tunable laser wavelength from 230–1100 nm [8]. One technology known for this application is an oscillator free-electron laser (FEL) [9–11], whose wavelength can be tuned by varying the undulator strength and the electron energy. However, tuning over this entire range continuously is not feasible because the high-reflectivity mirrors will need to be changed out for appropriate wavelength ranges.

A SEMI-CLASSICAL MODEL FOR RESONANT COMPTON SCATTERING

We use a semi-classical model to study resonant Compton scattering by treating the electron motion in the ion rest frame as a damped-driven oscillator [12]. The system is driven by the incident laser field and damped by the radiative reaction. We impose the angular momentum of the electron is quantized and posit that the damping mechanism only damps out small oscillations about the electron's stable orbit to avoid the quintessential problems of the classical model associated with orbital collapse.

We make the following assumptions about the laser light:

- the wavelength is long compared to the size of the ion,
- the incident field appears as a plane wave and position-dependent forces are averaged out, and
- the electron motion about the nucleus is circular and non-relativistic.

Under these conditions we find the differential scattering cross-section to be given by

$$\frac{d\sigma}{d\Omega} = r_e^2 \frac{\omega^4}{(\omega_0^2 - \omega^2)^2 + \Gamma^2\omega^2} \left|\epsilon \cdot \epsilon'^*\right|^2, \tag{5}$$

where ϵ and ϵ' are the polarization vectors of the incident and scattered photons, respectively, and ω is the angular frequency of the incident photon. The constant r_e is the classical electron radius, ω_0 is the angular frequency of the stable orbit, and the damping coefficient is $\Gamma = \frac{2r_e}{3c}\omega_0^2$.

Summing over the final polarizations in a plane transverse to the scattering direction and then integrating over all scattering directions yields the total scattering cross-section

$$\sigma_{\text{tot}}(\omega) = \sigma_T \frac{\omega^4}{(\omega_0^2 - \omega^2)^2 + \Gamma^2\omega^2}, \tag{6}$$

where $\sigma_T = \frac{8\pi}{3} r_e^2$ is the Thomson cross-section. In the low-frequency limit ($\omega \ll \omega_0$), the total cross-section scales as $\sigma \propto (\frac{\omega}{\omega_0})^4$, consistent with the fourth order dependency in Rayleigh scattering [12]. In the high-frequency limit ($\omega \gg \omega_0$), the electron behaves as a free electron and the total cross-section approaches σ_T, agreeing with conventional Compton scattering. However, at $\omega = \omega_0$, this cross-section exhibits a resonance where $\sigma_{\text{res}} = \sigma_T(\omega_0/\Gamma)^2 = \sigma_T Q^2$, where the Q-factor is $Q = \omega_0/\Gamma$. For the elements plotted in Fig. (2) (Z: 18–82), Q as determined by this classical model ranges from 10^4–10^2. This illustrates a great benefit of resonant Compton scattering, where on resonance, the scattering cross-section can be several orders of magnitude greater than that of conventional Compton scattering.

Effective Total Cross-Section

While resonant Compton scattering enables a significant increase in the scattering cross-section of individual interactions, the finite bandwidth of real beams will limit the achievable increase in gamma-ray flux. To illustrate this, consider an ion beam and a laser beam, which have energy and photon density distributions taken to be gaussian in the lab frame. The relative rms spreads are Σ_γ/γ_0 and $\Sigma_\omega^{\text{las}}/\omega_0^{\text{las}}$ for the ion and laser beam, respectively. Then, because of the linear mapping, the photon density distribution of the photons in the rest frames of the ions would become

$$f_{\text{laser}}(\omega) = \frac{1}{\sqrt{2\pi}\Sigma_\omega} \exp\left[-\frac{(\omega - \omega_0)^2}{2\Sigma_\omega^2}\right], \tag{7}$$

where $\Sigma_\omega/\omega_0 = \sqrt{(\Sigma_\gamma/\gamma_0)^2 + (\Sigma_\omega^{\text{las}}/\omega_0^{\text{las}})^2}$.

To quantify the interaction efficiency of the beams, we define an effective cross-section given by

$$\sigma_{\text{eff}} \equiv \int \sigma_{\text{tot}}(\omega) f_{\text{laser}}(\omega)\, d\omega, \tag{8}$$

ISBN: 978-3-95450-261-5 ISSN: 2673-7000 doi: 10.18429/JACoW-NAPAC2025-THP062

where $\sigma_{\text{tot}}(\omega)$ and $f_{\text{laser}}(\omega)$ are given by Eqs. (6) and (7), respectively. This integral has no closed-form analytical solution. Nevertheless, we can estimate σ_{eff} when two approximations are simultaneously applicable: (1) $f_{\text{laser}}(\omega)$ is mostly flat across the resonance, i.e. $Q \gg \frac{\omega_0}{\sqrt{2\pi}\Sigma_\omega}$ and (2) $\sigma_{\text{tot}}(\omega)$ is approximated well by a Lorentzian form due to $Q \gg 1$. Applying these, the effective cross-section can be expressed as

$$\sigma_{\text{eff}} \approx \left[\sqrt{\frac{\pi}{8}}\frac{\omega_0}{Q\Sigma_\omega}\right]\sigma_{\text{res}} = \alpha\sigma_{\text{res}}, \tag{9}$$

where α represents the efficiency of beam-beam scattering and is an overestimate due to the first approximation.

For example, let us consider the interaction of an Ar^{17+} ion beam with a laser. We take a central Lorentz factor that matches the angular frequency of the laser in the ion rest frame ω with the angular frequency of the lowest stable orbit ω_0. We assume realistic relative rms spreads of $\Sigma_\gamma/\gamma_0 = 10^{-4}$ [7] and $\Sigma_\omega^{\text{las}}/\omega_0^{\text{las}} = 10^{-3}$ [13]. The total cross-section $\sigma_{\text{tot}}(\omega)$ and photon density distribution in the ion rest frames $f_{\text{laser}}(\omega)$ for this example are plotted relative to their maximums in Fig. 3. For our parameters, the scattering efficiency is $\alpha \approx 5.2\%$. This demonstrates the significant loss of efficiency in scattering when most photons are not interacting resonantly with ions.

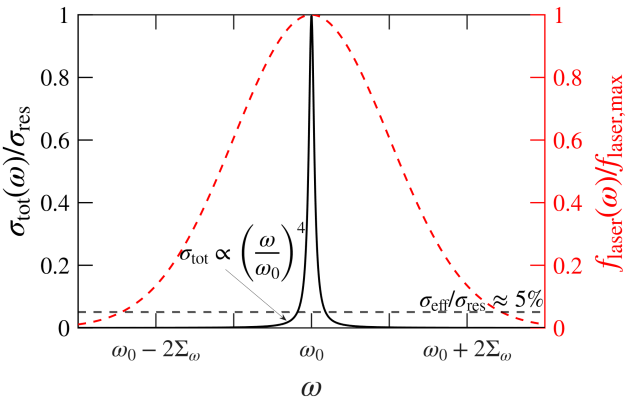

Figure 3: Total cross-section (left) and laser distribution as seen by the ion beam (right) plotted against frequency for Ar^{17+} ($Q \approx 1.2 \times 10^4$) with relative rms energy spread of 10^{-4}. The laser beam has a relative rms bandwidth of 10^{-3} that appears widened due to the ion distribution.

Quantum Mechanical Effects

The physics of photon absorption and emission by an atom is, at its core, a quantum mechanical phenomenon. A fundamental assumption made earlier is that the atom is a two-level system. With this assumption, the cross-section model presented earlier is expected to be useful for describing the actual quantum mechanical effects involved in resonant Compton scattering. Instead of using classical values, two main parameters in the model (Eqs. 6 and 7) need to be adjusted: (1) The resonant frequency ω_0 should be the angular frequency of the photon that excites the ion from the ground state to the excited state; (2) The linewidth parameter Γ should be based on quantum mechanical results, or preferably, be the measured values if available. The discrepancy between the semi-classical and quantum mechanical results are important. For example, for the hydrogen atom, the measured lifetime of the 2P state is longer than the classical value calculated using the stable orbit model of the ground state.

A Framework for Beam Scattering Simulation

Monte Carlo simulation codes have been developed for conventional Compton scattering to simulate beam-beam scattering [5]. We propose a framework to incorporate this semi-classical model into similar algorithms by separating the scattering physics from kinematics associated with the transformations between the lab and particle rest frames.

First, both the ion and laser beam distributions can be Lorentz transformed into the nominal ion rest frame. Then calculate the beam scattering based on a specific differential cross-section, while including the spatial and spectral dependencies. The resulting scattered beam is then transformed back to the laboratory frame. Working in the ion rest frame provides flexibility to replace the cross-section model as needed, for example, to include quantum mechanical effects.

SUMMARY AND DISCUSSION

In this work, we reviewed the kinematics of resonant Compton scattering, discussed the resonance condition, and the capabilities of resonant Compton scattering with examples of hydrogen-like ions. We developed a semi-classical model of the resonant interaction by treating the system as a damped-driven oscillator. This model was applied for the ion and laser beams of finite energy/linewidth distributions to estimate the effective total cross-section. We also discuss how this model can be modified to more accurately agree with observation by accounting for quantum mechanical effects. Last, we presented a framework to incorporate this model in scattering simulation code.

Our model assumes the laser beam has a continuous Gaussian spectral distribution. However, to achieve high laser power for scattering, a resonant power enhancement cavity is typically used in conjunction with a pulsed laser. The resulting spectral distribution is a narrow frequency comb enveloped by a Gaussian profile. Effort should be devoted to investigating the impact of frequency matching and the choice of resonant cavity parameters on the scattering efficiency, in order to optimize the overall performance of a resonant Compton gamma-ray source.

ACKNOWLEDGMENTS

This work was carried out at the High Intensity Gamma-ray Source facility at the Triangle Universities Nuclear Laboratory (TUNL).

ISBN: 978-3-95450-261-5 ISSN: 2673-7000 doi: 10.18429/JACoW-NAPAC2025-THP062

REFERENCES

[1] A. H. Compton, "A quantum theory of the scattering of x-rays by light elements", *Phys. Rev.*, vol. 21, no. 5, pp. 483–502, 1923. doi:10.1103/PhysRev.21.483

[2] H. R. Weller *et al.*, "Research opportunities at the upgraded HIgS facility", *Prog. Part. Nucl. Phys.*, vol. 62, no. 1, pp. 257–303, 2009. doi:10.1016/j.ppnp.2008.07.001

[3] M. W. Krasny, "The gamma factory proposal for CERN", 2015, arXiv:1511.07794 [hep-ex]. doi:10.48550/arXiv.1511.07794

[4] W. Płaczek *et al.*, "Gamma factory at CERN — novel research tools made of light", *Acta Phys. Pol. B*, vol. 50, no. 6, p. 1191, 2019. doi:10.5506/aphyspolb.50.1191

[5] C. Sun and Y. K. Wu, "Theoretical and simulation studies of characteristics of a compton light source", *Phys. Rev. Spec. Top. Accel Beams*, vol. 14, no. 4, 2011. doi:10.1103/physrevstab.14.044701

[6] G. Roland, K. Šafařík, and P. Steinberg, "Heavy-ion collisions at the LHC", *Prog. Part. Nucl. Phys.*, vol. 77, pp. 70–127, 2014. doi:10.1016/j.ppnp.2014.05.001

[7] M. Schaumann, "Potential performance for pb-pb, *p*-pb, and *p*−*p* collisions in a future circular collider", *Phys. Rev. ST Accel. Beams*, vol. 18, no. 9, p. 091 002, 2015. doi:10.1103/PhysRevSTAB.18.091002

[8] Y. K. Wu *et al.*, "Lasing below 170 nm using an oscillator fel", *J. Appl. Phys.*, vol. 130, no. 18, p. 183 101, 2021. doi:10.1063/5.0064942

[9] Y. K. Wu, N. A. Vinokurov, S. Mikhailov, J. Li, and V. Popov, "High-gain lasing and polarization switch with a distributed optical-klystron free-electron laser", *Phys. Rev. Lett.*, vol. 96, no. 22, p. 224 801, 2006. doi:10.1103/PhysRevLett.96.224801

[10] J. Yan *et al.*, "Precision control of gamma-ray polarization using a crossed helical undulator free-electron laser", *Nat. Photon.*, vol. 13, pp. 629–635, 2019. doi:10.1038/s41566-019-0467-6

[11] J. Yan *et al.*, "Polarization control of a free-electron laser oscillator using helical undulators of opposite helicities", *Phys. Rev. Accel. Beams*, vol. 23, no. 6, p. 060 702, 2020. doi:10.1103/PhysRevAccelBeams.23.060702

[12] J. D. Jackson, *Classical Electrodynamics, 3rd Edition*. 1998.

[13] C. Sun, J. Li, G. Rusev, A. P. Tonchev, and Y. K. Wu, "Energy and energy spread measurements of an electron beam by compton scattering method", *Phys. Rev. ST Accel. Beams*, vol. 12, no. 6, p. 062 801, 2009. doi:10.1103/PhysRevSTAB.12.062801